Atmospheric
Chemistry
and Physics

Characterising tropospheric O₃ and CO around Frankfurt over the period 1994–2012 based on MOZAIC–IAGOS aircraft measurements

Hervé Petetin, Valérie Thouret, Alain Fontaine, Bastien Sauvage, Giles Athier, Romain Blot, Damien Boulanger, Jean-Marc Cousin, and Philippe Nédélec

Laboratoire d'Aérologie, Université de Toulouse, CNRS, UPS, Toulouse, France

Correspondence to: Hervé Petetin (hervepetetin@gmail.com)

Abstract. In the framework of the MOZAIC–IAGOS programme, vertical profiles of ozone (O_3) and carbon monoxide (CO) have been available since 1994 and 2002, respectively. This study investigates the variability and trend of both species in three tropospheric layers above the German airports Frankfurt and Munich. About 21 300 flights have taken place over the period 1994–2012, which represents the worldwide densest vertical in situ data set of O_3 and CO (with ∼ 96 flights per month on average). The mean vertical profile of ozone shows a strong gradient in the first kilometre during the whole year and in the tropopause region in spring and summer. The mean vertical profile of CO is characterised by high mixing ratios at the ground, a strong decrease in the first kilometre, in particular in winter and autumn, and a moderate one in the free troposphere. O_3 minimises in November–December and shows a broad spring/summer maximum in the lower and mid-troposphere and a sharp maximum in summer in the upper troposphere. The seasonal variation of CO shows a broad minimum in July–October close to the surface and in September–October it occurs higher in the troposphere, while the maximum occurs in February–April in the whole troposphere. Over the period 1994–2012, O_3 has changed insignificantly (at a 95 % confidence level), except in winter where a slightly significant increase (from $+0.83\,[+0.13;+1.67]\,\%\,\mathrm{yr}^{-1}$ in the LT to $+0.62\,[+0.02;+1.22]\,\%\,\mathrm{yr}^{-1}$ in the UT, relative to the reference year 2000) is found. The O_3 5th percentile shows similar upward trends at the annual scale in all three tropospheric layers. All trends remain insignificant for the O_3 95th percentile. In contrast, for CO the mean as well as its 5th and 95th percentiles decrease both at the an-

nual scale and at the seasonal scale in winter, spring and summer (although not always in all three tropospheric layers) with trends ranging between $-1.22\,[-2.27;-0.47]$ and $-2.63\,[-4.54;-1.42]\,\%\,\mathrm{yr}^{-1}$, relative to the reference year 2004. However, all CO trends remain insignificant in autumn.

The phase of the seasonal variation of O_3 was found to change in the troposphere. The O_3 maxima moves forward in time at a rate of $-17.8\pm11.5\,\mathrm{days\,decade}^{-1}$ in the lower troposphere, in general agreement with previous studies. Interestingly, this seasonal shift is shown to persist in the mid-troposphere ($-7.8\pm4.2\,\mathrm{days\,decade}^{-1}$) but turns insignificant in the upper troposphere.

1 Introduction

As one of the major sources of hydroxyl radicals (OH) that directly control the atmospheric lifetime of a large number of compounds, ozone (O_3) plays a unique role in the oxidative capacity of the atmosphere. In the troposphere, it acts as a powerful greenhouse gas with a positive radiative forcing (RF) of $0.40\pm0.20\,\mathrm{W\,m}^{-2}$ that is not compensated by the RF of stratospheric ozone estimated at $-0.05\pm0.10\,\mathrm{W\,m}^{-2}$ (IPCC, 2013). It also has well-known adverse impacts on human health (Jerrett et al., 2009), vegetation (Ashmore, 2005; Paoletti, 2006) and agricultural crop yields (Van Dingenen et al., 2009). In the troposphere, O_3 is formed by photochemical reactions implying various compounds including volatile organic compounds (VOCs), carbon monoxide (CO) and nitrogen oxides (NO_x). It can be removed by

photolysis, dry deposition and uptake on aerosols (Moise and Rudich, 2000, 2002). Despite the considerable scientific achievements made during the last decades, the O_3 budget remains difficult to quantify precisely (Wu et al., 2007). Major uncertainties are related to lightning NO_x production, isoprene biogenic emissions and degradation chemistry, biomass burning emissions, water vapour concentrations and stratosphere–troposphere exchange (STE) (Stevenson et al., 2006). This leads to a large heterogeneity of the O_3 abundance and variability in the troposphere, making it difficult to draw a simple and global picture of the O_3 present-day concentrations and trends.

During the last decades, O_3 trends in the free troposphere have been intensively investigated, notably based on long-term ozonesonde observations. Specifically in Europe where such measurements are available over a few decades at several sites (e.g. Hohenpeissenberg, Payerne, Uccle, De Bilt, Legionowo, Lindenberg), most results indicate an increase in ozone levels from the 1960s to the mid-1980s (Logan et al., 1999; Oltmans et al., 1998; Tiao et al., 1986), the only site with no significant trend being Lindenberg, Germany, for the period 1975–1983 (Tiao et al., 1986). Such positive trends were found throughout the year without any significant seasonal influence (Logan et al., 1999) and through the entire tropospheric column (Logan et al., 1999; Oltmans et al., 1998). By the mid-1980s to 2000s, most ozonesonde observations in Europe indicated a progressive levelling-off of ozone mixing ratios in the free troposphere (Logan et al., 1999; Oltmans et al., 1998, 2006; Gaudel et al., 2015). For instance, the significant positive trends obtained at Hohenpeissenberg in the entire tropospheric column for 1971–2010 vanish in most tropospheric layers in the period 1981–2010 (Oltmans et al., 2013). Ozone observations at Jungfraujoch, Switzerland (3850 m), an elevated alpine site supposed to be representative of the free troposphere, indeed reveal that mixing ratios have continued to increase in the 1990s, in particular during winter, with the levelling-off occurring only in the 2000s (Cui et al., 2011). A similar evolution is reported by Cooper et al. (2014) at other mountain or remote sites in Europe and by Logan et al. (2012) on the observations by the MOZAIC (Measurement of Ozone and Water Vapor by Airbus in-service Aircraft) aircraft above some European airports.

Observations at the coastal site Mace Head have shown an average annual increase of $+0.25 \pm 0.09$ ppb yr^{-1} of the baseline (i.e. originating from the Northern Hemispheric marine boundary layer) O_3 mixing ratios during the period 1988–2012 (Simmonds et al., 2004; Derwent et al., 2013). This increase has been the strongest in winter and spring and the lowest in summer and has slowed down during the 2000s (Derwent et al., 2013). In contrast, the annual O_3 mixing ratios in European air masses have shown a much lower increase (Derwent et al., 2013), which suggests a possible compensation between a decrease of O_3 local formation in Europe and an increase of O_3 imports. At several remote or

alpine sites in northern midlatitudes, Parrish et al. (2013) recently highlighted a noticeable shift in the O_3 cycle at the ground, with the maximum daily O_3 occurring between 3 and 6 days earlier each decade since the 1970s. Such a shift may reflect some changes in the transport pathways, precursors emissions and photochemistry of O_3, possibly due to climate change (Parrish et al., 2013).

The present study aims at characterising the vertical distribution, the temporal variability, the seasonality and the trends of tropospheric O_3 in central/western Europe. Based on vertical profiles measured by commercial aircraft involved in the MOZAIC–IAGOS (In-service Aircraft for a Global Observing System) programme, it will focus on the free and upper troposphere in order to go beyond the more limited representativeness in the boundary layer (BL) at the regional scale. However, results in the BL will be also presented to give a full picture of the troposphere. This study will also investigate the variability and trend of CO, one of the main O_3 precursors measured in the framework of the MOZAIC–IAGOS programme. As a moderate lifetime (several weeks to several months) compound emitted by incomplete combustion processes, CO represents a powerful pollution tracer able to provide information on long-range transport at the hemispheric scale. Characterising CO in troposphere may thus help to investigate the variability and trend affecting O_3.

Section 2 presents the MOZAIC–IAGOS data set and describes the treatment applied to vertical profile data. The vertical distribution, the seasonal variations, the trends of O_3 and CO and the changes affecting the O_3 seasonal cycle are analysed in Sect. 3. The main results and conclusions are summarised in Sect. 4.

2 Data and methodology

2.1 MOZAIC–IAGOS data set

In the framework of the MOZAIC–IAGOS programme (http://www.iagos.org), O_3 and CO measurements (among other parameters) have been carried out by commercial aircraft along various flight routes in the world (most of them from or to European airports) since 1994 (O_3) and 2002 (CO), respectively (Marenco et al., 1998; Petzold et al., 2015). Until October 2014 (date of the last MOZAIC aircraft flight), both O_3 and CO have been measured using the same instruments in all aircraft, thus ensuring the data set consistency during most of the period. Ozone measurements were carried out using a dual-beam UV-absorption monitor (time resolution of 4 s) with an accuracy/precision estimated at about ± 2 ppbv/± 2 % (Thouret et al., 1998). Carbon monoxide was measured by an improved infrared filter correlation instrument (time resolution of 30 s) with an accuracy/precision estimated at ± 5 ppbv/± 5 % (Nédélec et al., 2003).

As MOZAIC aircraft have been retired from service, the European partners involved have been preparing the technical successor for the framework of the European Commis-

sion (EC)-funded IAGOS programme (Petzold et al., 2015) for years. A new concept of aircraft system and instruments has been developed and installed on Airbus long-range aircraft (A340 or A330), starting from July 2011. Seven aircraft are actually in operation with IAGOS systems. The new IAGOS instrumentation for O$_3$ and CO is extensively described in Nédélec et al. (2015). The O$_3$ and CO measurements are based on the same technology used for MOZAIC, with the same estimated accuracy and the same data quality control. Nearly 4 years overlap of "historical" MOZAIC and "new" IAGOS instrumentation allowed us to prove that the new IAGOS systems provide the same data quality (Nédélec et al., 2015), which is especially important for trends analysis.

Note also that several studies have investigated the consistency of the MOZAIC–IAGOS O$_3$ data set with other types of in situ data (e.g. surface stations, ozonesonde) (Logan et al., 2012; Staufer et al., 2013, 2014; Tanimoto et al., 2015; Zbinden et al., 2013). Focusing on O$_3$ changes in Europe, Logan et al. (2012) showed a reasonable agreement between aircraft and alpine sites but noticed the absence of O$_3$ increase in 1994–1998 in the sonde data set (contrary to the two other types of data). Focusing on the pure tropospheric profiles, Zbinden et al. (2013) found a mean difference between MOZAIC–IAGOS and sondes of -2 % in Germany, -8 % in eastern United Sates and $+1$ % over Japan. Tanimoto et al. (2015) obtained similar results, with differences between aircraft and sondes data around ± 2 % throughout the whole troposphere in Belgium, Germany and Japan and ± 5 % at Hong Kong. The MOZAIC–IAGOS data at Munich were found to compare reasonably well with the surface observations at Hohenpeissenberg (slope of 0.97, correlation of 0.77).

The present study will focus on Frankfurt Airport where the longest (from 1994 to 2012) and densest (18 598 flights) record is available. In order to fill a large data gap in 2005, this data set is combined to the data from the airport Munich (2734 flights, mostly between 2002 and 2005), approximately 300 km south-east of Frankfurt, as done in several previous studies (Logan et al., 2012; Zbinden et al., 2006, 2013). Note also that no measurements are available during part of 2010 due to instrumental problems. An illustration of the data set density by month and year is shown in Figs. S1 and S2 of the Supplement.

2.2 Tropopause altitude and tropospheric layers

This paper focuses on the analysis of tropospheric vertical profiles obtained over Europe (Germany) during both ascent and descent. As tropospheric O$_3$ shows strongly varying sources, sinks and lifetimes with height, here the troposphere is divided into three layers: the lower troposphere (LT), the mid-troposphere (MT) and the upper troposphere (UT). As in Thouret et al. (2006), the UT is defined here as the layer with its top at the tropopause plus 15 hPa and spanning a pressure of 60 hPa, i.e. a layer ~ 1.6 km thick and starting/ending

$\sim 2.1/\sim 0.5$ km below the tropopause. The MT is delimited by the UT lower boundary and an arbitrarily fixed altitude of 2 km. Data collected below are finally assigned to the LT. The first kilometre above the surface is ignored to limit the representativeness degradation induced by emissions over the airport area (confirmed by large enhancements of CO mixing ratios near the ground in most vertical profiles). The influence of the local emissions on the observations in the LT will be briefly discussed in Sect. 3.2.2.

The tropopause altitude can be estimated by several approaches, e.g. thermal, dynamic, chemical criteria (Thouret et al., 2006) or a combination of them (Stohl et al., 2003b). In this paper, we consider the dynamical tropopause (DT), delimited by a potential vorticity (PV) of 2 pvu (1 pvu $= 10^{-6}$ K m^2 kg^{-1} s^{-1}) (see the tropopause height over the period 1994–2012 in Fig. S3 of the Supplement). Two parameters, the PV and the pressure at which PV reaches 2 pvu (so-called $p_{\mathrm{PV}=2}$), are derived along all MOZAIC flight routes based on the European Centre for Medium-Range Weather Forecasts (ECMWF) operational analysis (00:00, 06:00, 12:00, 18:00 UTC) and forecasts (03:00, 09:00, 15:00, 21:00 UTC). The pressure at the DT ($p_{\mathrm{PV}=2}$) plus 15 hPa defined the top of the UT applied here.

Tropospheric vertical profiles are selected according to several criteria.

i. Distance from the airport: take-offs and landings do not exactly correspond to vertical profiles as aircraft travel some distance before reaching their cruise altitude. In order to limit the uncertainties induced by a potential horizontal heterogeneity, a maximum distance of 400 km from the airport is fixed for the vertical profile data selection. In practice, such a distance is sufficient for sampling the entire vertical profile in most flights and remains reasonable considering the fact that the O$_3$ vertical variability is expected to be higher than the horizontal one. A sensitivity test with a distance threshold of 800 km leads to differences of mean O$_3$ mixing ratio in the UT below 3 % at the seasonal and annual scale.

ii. Potential vorticity: based on PV vertical profiles, the 2 pvu value is used to locate the top of the tropospheric vertical profiles. This is illustrated in Fig. 1 with the flight from Frankfurt to Boston on 19 March 2002 during which the DT altitude is estimated at 8.8 km. If the distance criterion is fulfilled before reaching DT, the $p_{\mathrm{PV}=2}$ parameter is used to estimate the DT pressure (thus determining to which tropospheric layer points belong). However, PV values above 2 pvu may sometimes be encountered in the lower troposphere due to recent deep stratospheric intrusions or convective processes, before decreasing again below the 2 pvu threshold to the tropopause. To avoid a misevaluation of the DT altitudes in such cases, PV values are not considered point by point but over a window of several points – in our case, 60 points, which approximately corresponds to 1800 m
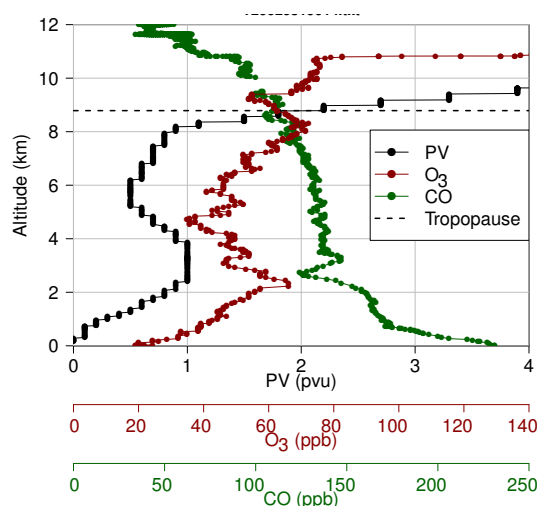
Figure 1. Vertical profile of the potential vorticity (PV), O_3 and CO mixing ratios during the flight from Frankfurt to Boston on the 19 March 2002 (take-off). The tropopause altitude (dotted black line) is estimated based on PV (see text for the methodology).

on the vertical – and the tropopause is considered to be reached only when the minimum PV over that window exceeds 2 pvu (this value of 60 being empirically chosen to handle most of these situations) (or when the previous criterion is fulfilled) and is set to the bottom of that window. In this study, we are thus considering the real and not pure tropospheric layer; i.e. recent stratospheric intrusions are not filtered in our methodology.

It is worth noting that the determination of the tropopause altitude is associated to several uncertainties. Some uncertainties arise from the choice of the method used to locate the tropopause. For instance, the chemical tropopause (defined in terms of both O_3 mixing ratio and vertical gradient of O_3 mixing ratio, also referred to as the ozone tropopause) is on average below the thermal tropopause (Bethan et al., 1996). In the determination of the DT altitude, other uncertainties can arise from the choice of a constant PV to locate the DT. Indeed, Kunz et al. (2011) showed that the PV values at the DT can vary between 1.5 and 5, with higher PV values in summer than in winter. In our case, there are also uncertainties related to the fact that here the PV is a modelled variable. In addition, it is linearly interpolated between PV fields 6 h apart, which does not allow us to entirely catch the variability of the DT. A good example is given in Fig. 1 where the abrupt O_3 increase (corresponding to the tropopause) occurs 2 km above the DT derived from PV values. However, our approach allows us to assess in which layer (MT or UT) observations belong even when the tropopause is not reached (within the 400 km around the airport).

In order to assess the uncertainties introduced by an erroneous DT pressure, we compared it with the chemical tropopause (CT), defined here as the pressure at which O_3

reaches the typical tropopause O_3 mixing ratios. In addition, we require that beyond that pressure, O_3 mixing ratios remain higher than these typical tropopause O_3 mixing ratios, in order to avoid a wrong determination due to stratospheric intrusions in the troposphere. As O_3 at the tropopause varies seasonally, we consider a dynamic criterion given by the formula $97 + 26 \times \sin((DayOfYear - 30) \times 2\pi/365)$ (ppb) proposed by Zahn et al. (2002) based on CARIBIC observations (and consistent with Thouret et al., 2006). We also require the CT to be located above the 600 hPa pressure level, in order to avoid a wrong allocation if for instance a high O_3 plume is sampled in the BL with missing data above in the profile. This was done for all vertical profiles where it was possible, which represents 41 % of the data set. On average over the period 1994–2012, the mean bias of the DT pressure compared to the chemical tropopause derived from O_3 mixing ratios is $+2$ hPa, while the 5th, 10th, 50th, 90th and 95th percentiles of this bias are -138, -57, $+10$, $+57$ and $+75$ hPa, respectively. Therefore, the DT pressure derived from PV does not appear systematically biased, but quite large discrepancies can exist on some profiles. It is beyond the scope of this study to investigate in more detail the influence of the method used to locate the tropopause. Above the airport Frankfurt, a majority of vertical profiles (63 %) reach the tropopause while most of the remaining profiles (36 %) are selected according to the distance criterion. A similar proportion is found at Munich (63 and 35 %, respectively).

2.3 FLEXPART simulations

The FLEXPART Lagrangian particle dispersion model (Stohl et al., 2005) is used to investigate the origin of air masses sampled by the aircraft in the different tropospheric layers above Frankfurt/Munich. Input meteorological data are taken from the ECMWF operational analysis (00:00, 06:00, 12:00, 18:00 UTC) and forecasts (03:00, 09:00, 15:00, 21:00 UTC) and interpolated on a $1° \times 1°$ global longitude-latitude grid. The methodology used here basically consists of releasing 1000 particles every 10 hPa along each vertical profile and following them backwards in time for 20 days. This duration corresponds approximately to the time during which a pollution plume is expected to remain significantly higher than the tropospheric background (Stohl et al., 2003a). The FLEXPART model computes the particles' residence time, sometimes referred to as the potential emissions sensitivity (PES), which is the potential to catch up emissions from certain regions. Outputs are given on a $1° \times 1°$ global longitude-latitude grid, over 1 km width vertical layers up to 11 km plus a remaining layer ranging from 11 to 50 km (i.e. 12 vertical layers). The PES between 0–1 km is presented in Fig. 2 for each tropospheric layer, averaged over the period 1994–2012. As expected, air masses sampled in the LT spend most of their time in the European BL (mostly in France, Germany, Benelux, the UK). In the MT, the influence of Europe persists but the influence of North America is greatly
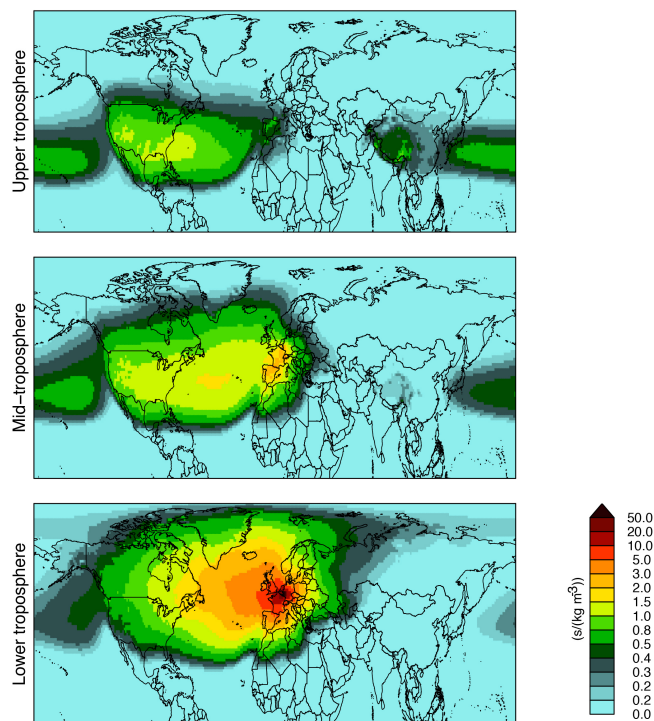
Figure 2. Average residence time in the first kilometre (normalised by the air density) of air masses sampled in all three tropospheric layers around Frankfurt. The average is calculated based on all FLEXPART simulations over the period 1994–2012. Note the irregular scale.

enhanced. In the UT, the PES is the highest over North America but stronger winds at these altitudes (e.g. jet streams) also allow for a fast transport of air masses from Asia.

3 Results

The climatological vertical profiles of O$_3$ and CO around Frankfurt/Munich are described in Sect. 3.1. The annual and monthly variations of both compounds are analysed in Sect. 3.2. The annual and seasonal trends are investigated in Sect. 3.3. The changes of the O$_3$ seasonal cycle are explored in Sect. 3.4.

3.1 Climatological vertical profiles

3.1.1 Ozone

Annual and seasonal mean vertical profiles of O$_3$ and CO are calculated over the whole period (1994–2012 for O$_3$, 2002–2012 for CO) and shown in Fig. 3. The standard deviation shown in Fig. 3 is inferred from the daily mean vertical profiles, thus representing the day-to-day variability at the seasonal scale. Over the entire tropospheric column, the annual mean O$_3$ mixing ratio is 56 ppb. The mean O$_3$ over the tropospheric column shows the minimum mixing ratios in win-

ter (44 ppb) and autumn (48 ppb), and the maximum ones in summer (67 ppb) and spring (61 ppb). The annual mean O$_3$ mixing ratio increases with altitude, from 21 ppb at ground to 81 ppb at 12 km (47 ppb at 2 km). The highest vertical gradients are found close to the surface during the whole year and close to 12 km during spring and summer. The inflexion of vertical gradients at about 1 km a.g.l. has already been mentioned in Chevalier et al. (2007). Above 3 km, the mean vertical gradients are $+1.1$, $+1.5$, $+3.0$ and $+5.1$ ppb km^{-1} in winter, autumn, spring and summer, respectively.

During the summer, short episodes of high O$_3$ mixing ratios are often observed in the European BL (van Loon et al., 2007; Meleux et al., 2007). High O$_3$ mixing ratios are also measured in urban environments, despite the presence of NO$_x$ emitted locally by anthropogenic activities (e.g., Vautard et al., 2001; Dueñas et al., 2002). Thus, one might have expected higher mixing ratios in the BL than in the lower free troposphere (sometimes described as a C-shaped profile), as sometimes observed in the profile above polluted cities (Ding et al., 2008; Tressol et al., 2008). However, observations do not show such a profile. One may suspect that this is due to the night-time titration of O$_3$ in the BL but limiting data to the afternoon does not highlight a clear C-shaped profile. Actually, such a C-shaped profile is only observed when considering the 95th percentile rather than the mean O$_3$ mixing ratio (Petetin et al., 2016). It means that the potentially high O$_3$ pollution in the BL during the summer can greatly modify the vertical profile of O$_3$ mixing ratios but only episodically. On average, the structure of the mean O$_3$ vertical profile in summer remains qualitatively the same (i.e. positive gradient through the whole troposphere) as during the rest of the year.

To further characterise the variability of O$_3$ and CO above Frankfurt/Munich, we now investigate the day-to-day variability at both the annual and seasonal scales. The day-to-day variability is here defined as the coefficient of variation (CV) of the daily averaged mixing ratios, which is the standard deviation normalised by the corresponding (i.e. annual or seasonal) mean mixing ratio. Vertical profiles of the day-to-day variability for O$_3$ and CO are shown in Fig. 4. Results about CO will be discussed in Sect. 3.1.2. The day-to-day variability of O$_3$ at the annual scale ranges between 20 and 73 % depending on the altitude, with a mean value of 32 %. The maximum day-to-day variability of O$_3$ is found at ground (73 %) and at 12 km (53 %), where it is likely driven by intense shallow and transient exchange between the stratosphere and the troposphere (Stohl et al., 2003b). Conversely, the minimum day-to-day variability is found at about 3.4 km. Such day-to-day variability is lower at the seasonal scale, at most altitudes and during most seasons, but the shape of the vertical profiles remains similar. The seasonal day-to-day variability minimises at 4.4 km in autumn and between 3.1–3.4 km in the other seasons, thus it is close to the minimum annual diurnal variability. Similarly, it maximises at the surface and close to the tropopause. Interestingly, the day-to-day variability above 11 km is noticeably higher in spring than during
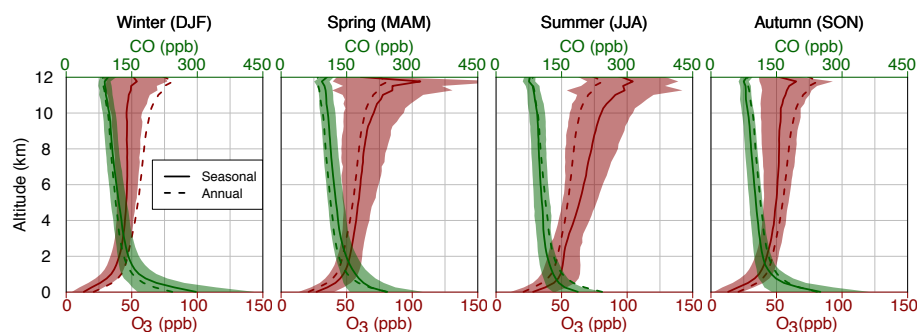
Figure 3. Climatological vertical profiles of O_3 and CO mixing ratios above Frankfurt/Munich per season (continuous lines). Standard deviation inferred from daily averaged profiles is also indicated (filled contour), as well as the annual mean profile (dotted line, the same for all panels).
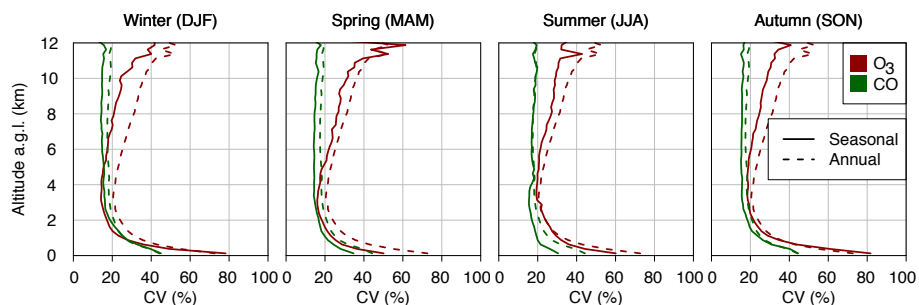

Figure 4. Annual (dotted lines, the same for all panels) and seasonal (continuous lines) day-to-day variability of O_3 and CO mixing ratios above Frankfurt/Munich. The day-to-day variability is defined here as the coefficient of variation (CV) of the daily averaged mixing ratios (i.e. the standard deviation normalised by the mean).

the other seasons, which again may be due to the day-to-day variability of STE that peaks during that season.

3.1.2 Carbon monoxide

The annual mean vertical profile of CO (Fig. 3) shows mixing ratios ranging from 150 ppb at 1 km to 80 ppb at 12 km. Over the entire tropospheric column, the mean CO mixing ratio is 117 ppb. At the ground and close to surface emissions, CO maximises with 243 ppb on the annual average. This high mixing ratio is first and foremost due to emissions from the airport area (including aircraft emissions on runways) and potentially due to emissions from the neighbouring agglomeration. The strongest seasonal variation is observed close to the surface, with mean mixing ratios in the first kilometre ranging from 156 ppb in summer to 233 ppb in winter. This increase during winter is likely due to higher emissions and a lower vertical mixing.

Figure 4 shows that the day-to-day variability is lower for CO than for O_3, in particular at the surface and close to the tropopause. Over the entire tropospheric column, the annual day-to-day variability of CO is 20 %. It ranges between 44 % close to the surface and 17 % in the free troposphere where it remains almost constant with altitude. A very similar picture is drawn for the different seasons. The highest values at the

surface (in the second half of the troposphere) are encountered in winter/autumn (summer).

3.2 Annual and monthly variations

The average seasonal variations of O_3 and CO in all three tropospheric layers around Frankfurt/Munich are given in Fig. 5 and their long-term time series are shown in Fig. 6.

3.2.1 Ozone

As noted in Sect. 3.1.1, the mean tropospheric O_3 increases with altitude, with average mixing ratios (over the whole period) of 44, 53 and 63 ppb in the LT, MT and UT, respectively. A clear seasonal pattern is emphasised in the entire tropospheric column. In the LT, the seasonal variation shows a broad spring/summer maximum and a minimum in winter, in good accordance with the seasonal variations observed at the surface in Europe (Wilson et al., 2012). In the MT and UT, mixing ratios maximise between May and August. The O_3 5th percentile shows higher mixing ratios in April–May in the LT and MT while the seasonal variations in the UT remains similar than for the mean O_3. The 95th percentile shows a maximum in spring/summer in all tropospheric layers, but is sharper in the UT than in the LT and MT.
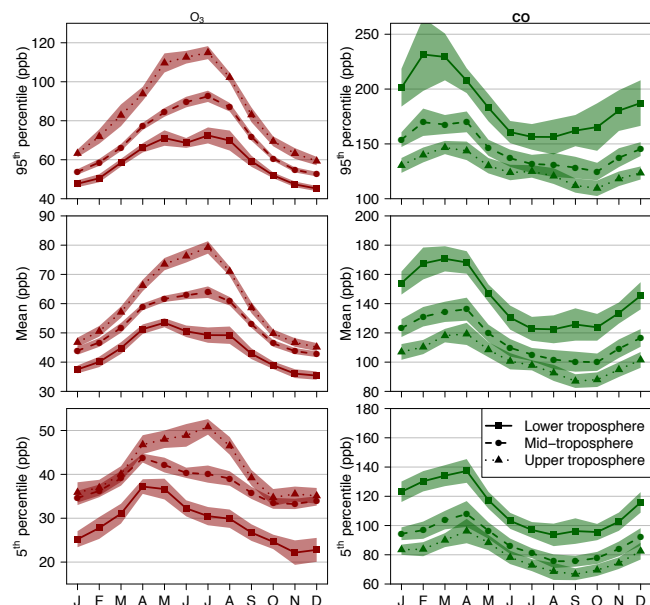
Figure 5. Averaged O$_3$ (left panels) and CO (right panels) seasonal variations above Frankfurt/Munich in all three tropospheric layers, for the 95th percentile (top panels), the mean (middle panels) and the 5th percentile (bottom panels). The shaded areas show the ±2 standard error (i.e. the uncertainty in the average at a 95 % confidence level) calculated based on the monthly averages assumed to be well determined (i.e. uncertainties on the individual monthly averages are not taken into account) and independent.

The annual mean O$_3$ mixing ratios are highly correlated between the three tropospheric layers ($R = 0.87$, 0.75 and 0.94 between the LT/MT, LT/UT and MT/UT, respectively). As the sources and sinks of O$_3$ in the troposphere strongly vary with altitude, such high correlations were not expected. This may be explained by the fact that both the first kilometre and the tropopause layer are not taken into account in this study, which likely reduces the differences of interannual variation among the tropospheric layers as defined in this study. However, some high O$_3$ mixing ratios are still observed in the UT, for instance with a 95th percentile up to 115 ppb in summer, which suggests an influence of stratospheric air. They are likely partly due to a wrong estimation of the tropopause height since we saw in Sect. 2.2 that, despite a very low mean bias, quite large differences can be found compared to a chemical tropopause determined based on typical tropopause O$_3$ mixing ratios. As we do not consider a purely tropospheric UT (see Sect. 2.2), some of these high O$_3$ mixing ratios may also be due to stratospheric intrusions in the troposphere. Similar correlations are obtained at the seasonal scale. An interesting exception is the low correlation found between the LT and UT in summer ($R = 0.26$) and spring (0.46). This may be due to the fact that the BL is deeper during these seasons (typically up to 3 km), which limits the influence of the free troposphere on the 1–2 km LT.

The highest monthly mean mixing ratios in the LT (above 60 ppb, the 99th percentile) are observed in August 1995, May 1998, August 2003, July 2006 (Fig. 6). The spring 1998 anomaly is related to the 1997 El Niño that enhanced the pollution export from Asia (due to a higher convective activity and a strengthening of the subtropical jet stream) and North America and may have increased the STE (Koumoutsaris et al., 2008; Zeng and Pyle, 2005). This anomaly is visible in the whole troposphere and is the strongest in the UT. The anomalies in August 2003 and July 2006 are related to the severe heat waves that struck a large part of Europe (Ordóñez et al., 2005; Solberg et al., 2008; Struzewska and Kaminski, 2008; see also Tressol et al., 2008 for a detailed analysis of the 2003 heat wave with the MOZAIC measurements). They are the strongest in the LT but remain visible in the MT.

3.2.2 Carbon monoxide

On average, CO mixing ratios of 143, 115 and 101 ppb are found in the LT, MT and UT, respectively. Mixing ratios in the UT are thus only 29 % lower than in the LT close to local emissions. In comparison with O$_3$, the monthly mean of the day-to-day variability of CO is lower and similar in all three tropospheric layers (around 14–16 %). Such a result is expected due to the longer lifetime of CO in comparison with O$_3$ in most of the troposphere, which leads to a higher regional and hemispheric background (Junge, 1974). As shown in Fig. 5, the seasonal cycle of CO is characterised by maximum mixing ratios in late winter/early spring in the whole troposphere. Minimum mixing ratios are encountered in summer/early autumn in the LT and are slightly shifted to late summer/early autumn higher in altitude. Such a seasonal pattern is consistent with the seasonal variation observed in background air masses arriving at the coastal site Mace Head (Derwent et al., 1998) or at a larger scale by satellite observations (Edwards et al., 2004; Worden et al., 2013). Averaged over western Europe, the Terra/MOPITT CO tropospheric column maximises at $\sim 2.5 \times 10^{18}$ molecules cm^{-2} in March–April and minimises at $\sim 1.9 \times 10^{18}$ molecules cm^{-2} in late summer, the ratio of the maximum over the minimum being 1.3 (Edwards et al., 2004). A very similar seasonal variation of tropospheric columns of CO has been observed by Zbinden et al. (2013) based on the MOZAIC data over the period 2002–2009. This is in good agreement with the amplitude of the seasonal cycle observed in the MT, the maximum CO mixing ratio being 1.35 higher than the minimum. The late winter/early spring maximum results from the accumulation of the primary CO emissions at northern midlatitudes when the oxidation by OH is limited. In summer, CO mixing ratios minimise due to a more effective photolytic destruction, despite an enhanced secondary formation from biogenic compounds and additional emissions from biomass burning (in particular in boreal regions). A rather similar seasonal pattern is observed with the CO 5th and 95th percentiles ex-
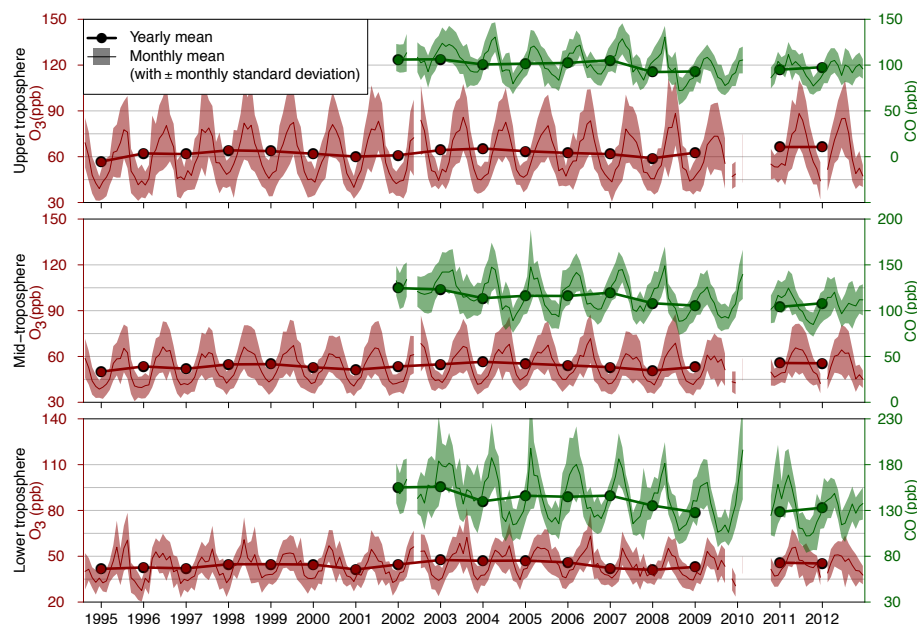
Figure 6. Monthly and yearly mean O$_3$ and CO mixing ratios of combined Frankfurt and Munich vertical profiles in the lower (bottom panel), middle (middle panel) and upper troposphere (top panel) between 1994 and 2012.

cept that the peak is sharper (February–March) in the LT for the 95th percentile.

As mentioned in Sect. 2.2 and 3.1.2, the data below 1 km were skipped in order to reduce the impact of the local emissions from both the neighbouring agglomeration and the other aircraft – on tarmac and/or during the take-off/landing phases (in case the MOZAIC–IAGOS aircraft closely follows other aircraft). Indeed, many studies have shown that airport activities can impact the air quality at the local scale (e.g. Hu et al., 2009; Pison and Menut, 2004; Yu et al., 2004). It is worth mentioning that in a standard landing take-off cycle – comprising the approach, the taxi (plane on the tarmac), the take-off (acceleration phase on the tarmac) and the climb up to a standard atmospheric boundary layer of 915 m (Kesgin, 2006) – most of the CO emissions (85–95 %) occur on the tarmac during the taxi phase (Kurniawan and Khardi, 2011). However, even above 1 km in the LT, one cannot exclude any influence of these emissions or the emissions of the neighbouring agglomeration.

To assess the spatial representativeness of the MOZAIC–IAGOS data in the LT and MT more precisely, a comparison is made with the CO mixing ratios measured at the World Meteorology Organization (WMO) Global Atmosphere Watch (GAW) surface stations (see Sect. S1 of the Supplement for details). Only the stations located between 45 and 55° N (i.e. ±5° from the latitude of Frankfurt) and with at least 80 % data capture for the period 2002–2012 (based on the monthly time series) are retained, which gives a set of 10 stations. The annual mean CO mixing ratio measured by MOZAIC–IAGOS aircraft in the LT (143 ppb) is in

the lower range of the zonal average 155 ± 28 ppb observed among the GAW surface stations. When considering only the stations above 1000 m (i.e. three stations, all located in Europe), the zonal average is reduced to 145 ± 19 ppb, which is very close to the mean CO observed in the LT. In the MT, the annual mean CO mixing ratio is 115 ppb, thus lower than the CO mixing ratios at the ground regardless of the station, but the difference for the highest mountain station Jungfraujoch (3580 m elevation) is very small (−7 %). Additionally, the annual MOZAIC–IAGOS CO data in both the LT and MT are strongly correlated with the CO observed at the ground (R between 0.61 and 0.94 at all stations except one at which $R = 0.41$). Therefore, the comparison between the MOZAIC–IAGOS CO data set at Frankfurt/Munich and the GAW data set at the same latitude shows good consistency, both in terms of mean annual CO mixing ratios and interannual variations. This ensures satisfactory representativeness of the MOZAIC–IAGOS observations.

For the period 2002–2012, the highest CO annual mixing ratios are encountered in 2003. This is in agreement with the satellite measurements that show a high positive anomaly on CO total columns in Europe and more generally in the Northern Hemisphere for this year, notably due to intense boreal fires (Worden et al., 2013). High mixing ratios in the LT are also observed during the winter of 2010, concomitantly with a cold snap over Europe that may have induced higher CO emissions (because of the residential heating) (Cattiaux et al., 2010).

3.3 Trends

In order to easily compare trends between the different tropospheric layers, O_3 mixing ratios are normalised following the approach of Parrish et al. (2014): (i) a quadratic least-squares regression is applied to mean annual mixing ratios in which the year 2000 is taken as a reference (i.e. the origin of the time series), (ii) the obtained intercept corresponds to the interpolated mean annual O_3 mixing ratio in 2000 (hereafter designated as $O_{3,2000}$) and is used for the normalisation. The year 2000 is chosen in order to facilitate the comparison with the results obtained by Parrish et al. (2014). Trends are thus expressed in percentage of year 2000 intercept per year (hereafter referred to as $\%O_{3,2000}\,\text{yr}^{-1}$). The same approach is used for each season. Considering the relatively short time coverage of MOZAIC–IAGOS observations (in comparison with measurements at some historical surface sites traditionally used for long-term trend calculations), we limit the analysis to linear regressions. Besides mean O_3 mixing ratios, we also investigate trends of the 5th and 95th percentiles. Hereafter, all these quantities are referred to as $M(O_3)$, $P_5(O_3)$ and $P_{95}(O_3)$ for clarity. The same approach is followed for CO, with the year 2004 as a reference (and the results expressed in $\%CO_{2004}\,\text{yr}^{-1}$). This year is chosen because in all three tropospheric layers, the mean CO mixing ratios in 2004 (140, 114 and 101 ppb in the LT, MT and UT, respectively) are very close to the mean CO mixing ratios over the period 2002–2012 (141, 114 and 102 ppb). Ozone and CO normalised mean mixing ratios at the annual and seasonal scale are shown in Fig. S4 of the Supplement (similar plots of the 5th and 95th percentile are given in Fig. S5–S6 of the Supplement).

Trends are investigated using the non-parametric Mann–Kendall analysis combined with Theil–Sen slope estimate (Sen, 1968), which has several important advantages compared to the least-square regression, including the absence of distributional assumptions and the lower sensitivity to outliers. We use the OpenAir package (in the statistical programming language R) developed for applications in atmospheric sciences (Carslaw and Ropkins, 2012). This package provides an estimation of the uncertainties based on the bootstrap method and allows us to take into account the autocorrelation of the data. The autocorrelation of environmental parameters is quite common (although often ignored in trend analysis) and tends to artificially decrease the uncertainties of trends, which can lead to the identification of trends that are actually insignificant (Weatherhead et al., 2002). Note that, using our approach, the confidence intervals are not necessarily symmetric (around the mean slope estimate). The Theil–Sen slope estimates are reported for CO in Table 1. The trend uncertainties obtained for O_3 and CO by ignoring the autocorrelation are reported in Table S1 of the Supplement.

3.3.1 Ozone

All annual and seasonal trends of the $M(O_3)$ appear insignificant, except in winter when a weakly significant increase is found in all three tropospheric layers ($+0.83\,[+0.13;+1.67]$, $+0.62\,[+0.05;+1.22]$ and $+0.62\,[+0.02;+1.22]\,\%O_{3,2000}\,\text{yr}^{-1}$ in the LT, MT and UT, respectively). Previous trend analysis at the alpine sites (Zugspitze since 1978, Jungfraujoch and Sonnblick since 1990) have highlighted (i) a strong increase of O_3 during all seasons in the 1980s (around $+0.6$–$0.9\,\text{ppb}\,\text{yr}^{-1}$), (ii) a persistent but lower increase in the 1990s during all seasons except summer where O_3 has levelled off, (iii) the extension of that levelling off in the 2000s to the other seasons and a slight decrease in summer (Logan et al., 2012; Parrish et al., 2012). This picture is in general agreement with our results in the lower part of the troposphere. More specifically, in winter, Parrish et al. (2012) found an average trend of $+0.61\pm0.25\,\%O_{3,2000}\,\text{yr}^{-1}$ at regional background sites in Europe over the last 2–3 decades, which is consistent with the trends found here over the period 1994–2012. At low altitudes, this increase of O_3 in winter is mainly attributed to a reduced O_3 titration by NO due to decreasing NO_x emissions (e.g. Ordóñez et al., 2005). The persistent positive trends found at higher altitudes suggest that wintertime O_3 has increased at a large scale (if not hemispheric) since air masses sampled by MOZAIC–IAGOS aircraft in both the MT and UT can be influenced by emissions from North America and Asia (as shown in Fig. 2).

Concerning the $P_5(O_3)$, a significant increase is found at the annual scale in all three tropospheric layers ($+1.03\,[+0.36;+1.62]$, $+0.42\,[+0.09;+0.68]$ and $+0.63\,[+0.09;+0.99]\,\%O_{3,2000}\,\text{yr}^{-1}$ in the LT, MT and UT, respectively). Conversely, trends of the $P_{95}(O_3)$ are all insignificant. Note that ignoring the autocorrelation of the data leads to some additional significant positive trends, including the $M(O_3)$ at the annual scale, the $P_5(O_3)$ in winter and autumn and the $P_{95}(O_3)$ in winter, although not in all tropospheric layers (see Table S1 of the Supplement). It is beyond the scope of this study to investigate why the autocorrelation has a stronger effect on these specific seasons or layers, but this illustrates the strong influence of the serial dependence on the trend analysis and the necessity of taking it into account.

3.3.2 Carbon monoxide

As previously mentioned in the beginning of Sect. 3.3, here CO trends are investigated relative to the reference year 2004. Over the period 2002–2012, the $M(CO)$ at the annual scale significantly decreases in the whole troposphere, with trends of $-1.51\,[-2.42;-0.44]$, $-1.55\,[-2.34;-0.72]$ and $-1.36\,[-2.05;-0.74]\,\%CO_{2004}\,\text{yr}^{-1}$ in the LT, MT and UT, respectively. Similar negative trends are also obtained for the $P_5(CO)$ and $P_{95}(CO)$ in all tropospheric layers. At

Table 1. Annual and seasonal trends of mean CO mixing ratios, 5th and 95th percentiles over the period 2002–2012. Trends are estimated using the Theil–Sen slope estimate (see text). Uncertainties are given at the 95 % confidence level (NS is a non-significant trend).

Season	Layer	CO relative trend ($\%\mathrm{CO}_{2004}\,\mathrm{yr}^{-1}$)			CO absolute trend ($\mathrm{ppb}\,\mathrm{yr}^{-1}$)		
		Mean	5th	95th	Mean	5th	95th
Year	UT	−1.36 [−2.05; −0.74]	−1.22 [−2.27; −0.47]	−1.43 [−2.08; −0.89]	−1.42 [−2.14; −0.78]	−0.91 [−1.69; −0.35]	−2.00 [−2.90; −1.24]
Year	MT	−1.55 [−2.34; −0.72]	−1.57 [−2.52; −0.68]	−1.44 [−2.25; −0.59]	−1.85 [−2.79; −0.85]	−1.33 [−2.15; −0.58]	−2.30 [−3.59; −0.95]
Year	LT	−1.51 [−2.42; −0.44]	−1.59 [−2.58; −0.46]	−1.41 [−2.40; −0.12]	−2.24 [−3.59; −0.65]	−1.69 [−2.75; −0.49]	−2.90 [−4.91; −0.25]
Winter	UT	−1.64 [−2.73; −0.80]	−1.39 [−2.76; −0.39]	−1.59 [−2.59; −1.06]	−1.84 [−3.06; −0.89]	−1.22 [−2.42; −0.34]	−2.20 [−3.60; −1.47]
Winter	MT	−1.50 [−2.53; −0.60]	−1.69 [−2.81; −0.31]	−1.22 [−2.24; −0.28]	−1.96 [−3.29; −0.78]	−1.68 [−2.80; −0.31]	−2.00 [−3.66; −0.45]
Winter	LT	NS	NS	NS	NS	NS	NS
Spring	UT	−1.67 [−2.83; −0.48]	NS	−1.97 [−3.13; −0.86]	−2.02 [−3.43; −0.58]	NS	−2.92 [−4.65; −1.28]
Spring	MT	−2.00 [−2.97; −0.69]	NS	−2.01 [−2.71; −1.07]	−2.76 [−4.09; −0.95]	NS	−3.45 [−4.66; −1.85]
Spring	LT	−1.91 [−2.72; −1.09]	NS	−2.22 [−4.04; −0.87]	−3.26 [−4.64; −1.86]	NS	−4.94 [−9.00; −1.94]
Summer	UT	NS	NS	−1.53 [−2.22; −0.59]	NS	NS	−1.94 [−2.83; −0.75]
Summer	MT	−1.83 [−3.25; −0.56]	NS	−2.29 [−3.77; −1.21]	−2.01 [−3.58; −0.62]	NS	−3.22 [−5.30; −1.70]
Summer	LT	−2.31 [−3.61; −0.97]	−2.08 [−2.83; −0.76]	−2.63 [−4.54; −1.42]	−3.08 [−4.81; −1.29]	−2.16 [−2.94; −0.79]	−4.45 [−7.69; −2.40]
Autumn	UT	NS	NS	NS	NS	NS	NS
Autumn	MT	NS	NS	NS	NS	NS	NS
Autumn	LT	NS	NS	NS	NS	NS	NS

the seasonal scale, the M(CO) and P_{95}(CO) show negative trends in winter, spring and summer, although not always in all tropospheric layers, while the P_5(CO) significantly decreases in winter (in the MT and UT) and summer (in the LT). Conversely, all trends in autumn are insignificant. Note that, when the autocorrelation of the data is not taken into account, the results show significant negative trends of the P5 (CO) in most layers and during all seasons, except autumn (see Table S1 of the Supplement). These results are in general agreement with previous studies in Europe (e.g. Karlsdóttir et al., 2000; Novelli et al., 2003; Dils et al., 2011; Worden et al., 2013). Based on satellite observations, Worden et al. (2013) highlighted a decrease of the total column of CO over Europe, around $-1.44 \pm 0.22\,\%\,\mathrm{yr}^{-1}$ with MOPITT over 2001–2011 and $-1.00 \pm 0.33\,\%\,\mathrm{yr}^{-1}$ with AIRS over 2003–2011, which is in the range of our results over Frankfurt. Over the period 1995–2007, Gilge et al. (2010) found trends of -3.36 ± 1.08 and $-1.51 \pm 0.64\,\mathrm{ppb}\,\mathrm{yr}^{-1}$ (reduced to $-2.65 \pm 0.04\,\mathrm{ppb}\,\mathrm{yr}^{-1}$ by filtering the background values; Zellweger et al., 2009) at two alpine sites from the WMO GAW network, in reasonable agreement with our absolute Theil–Sen slope estimates at Frankfurt/Munich in the LT and MT ($-2.24\,[-3.59; -0.65]$ and $-1.85\,[-2.79; -0.85]\,\mathrm{ppb}\,\mathrm{yr}^{-1}$).

3.4 Changes of the O₃ seasonal cycle

In Sect. 3.3.1, we highlighted that only a few O₃ trends are statistically significant. However, the differences of trends between the seasons remain insignificant. It is worth noting that an insignificant trend does not imply the absence of trend since a trend can be hidden by a strong variability. In this section, we investigate whether these trends are linked to a change in the O₃ seasonal cycle above Frankfurt/Munich (Sect. 3.4.1). The results are discussed in Sect. 3.4.2.

3.4.1 Evolution of the seasonal cycle at Frankfurt/Munich

The seasonal variation of O₃ can be well approximated by a sine function fully characterised by three parameters: an offset value defined here as the average O₃ mixing ratio over the considered period, an amplitude and a phase that determines at which period in the year the maximum of O₃ is reached. Following the approach of Parrish et al. (2013), one can fit a sine function over different periods of time and compare the results of the fit in order to highlight potential changes in the seasonal pattern of O₃. While Parrish et al. (2013) applied the sine fit to the monthly mean time series, here we consider the daily mean O₃ mixing ratio. The equation of the fit is

$$\widetilde{y}(t) = y_0 + a \sin\left(\frac{2\pi t}{365} + \phi\right), \tag{1}$$

with t as the time (in days, values ranging between 0.5 and 364.5), y_0 the offset mixing ratio (in ppb), a the amplitude

(in ppb) and ϕ the phase. The day of the year of the seasonal maximum of O₃ is then estimated as $(\pi/2 - \phi) \times 365/2\pi$ (Parrish et al., 2013). We apply the sine fit to the two 9-year time periods 1995–2003 and 2004–2012. As there is no overlap between these periods, the two data sets and the results of the sine fit are independent. The changes of amplitude and phase obtained with the sine fits are reported in Table 2. The uncertainties directly given by the standard linear least-square regression are underestimated since daily averages of O₃ show some synoptic-scale multi-day correlation (readily seen in the correlograms of the daily residuals of the sine fits, not shown). In order to take into account this autocorrelation in the estimation of the uncertainties, we assume that the data follow a first-order regressive process, which allows us to estimate the effective independent sample size (n') based on the sample size (n) and the lag-1 autocorrelation coefficient (ρ_1): $n' = n(1 - \rho_1)/(1 + \rho_1)$ (Wilks, 2006). These lag-1 coefficients for the two periods and the three layers range between 0.22 and 0.60, which leads to an increase of the initial confidence intervals by a factor of 1.3 to 2.0. The uncertainties (95 % confidence interval) reported in Table 2 reflect this calculation.

Between the averages of the periods 1995–2003 and 2004–2012, the amplitude of the O₃ seasonal cycle has decreased at levels that are statistically significant throughout the troposphere, with differences of -2.5 ± 1.7, -1.1 ± 0.8 and $-2.1 \pm 1.2\,\mathrm{ppb}\,\mathrm{decade}^{-1}$ in the LT, MT and UT, respectively. Note that the difference between the two 9-year periods has been scaled to per decade. The reason for the decreasing amplitude is the significantly increased yearly O₃ minimum occurring in winter whereas the maximum occurring in spring/summer remained constant (see Sect. 3.3.1). The differences of amplitude change between the different layers are all statistically insignificant.

Over the period 1995–2003, the sine fit gives a seasonal maximum of O₃ on 18 June in the LT and on 23 June in the MT and UT. The date of seasonal maximum in the LT is in reasonable agreement with those obtained by Parrish et al. (2013) at two alpine sites (Jungfraujoch, Switzerland and Zugspitze, Germany) and at a lower elevation site (Hohenpeissenberg, Germany, $\sim 50\,\mathrm{km}$ from Munich). Over the period 2004–2012, the seasonal maximum O₃ occurs on 2 June in the LT, on 16 June in the MT and on 20 June in the UT. Thus, the phase of the seasonal variations of O₃ shifted forward during the period 1995–2012. The shift of the O₃ maximum (typically in June) between the averages of the periods 1995–2003 and 2004–2012 is statistically significant in the LT ($-17.8 \pm 11.5\,\mathrm{days}\,\mathrm{decade}^{-1}$) and MT ($-7.8 \pm 4.2\,\mathrm{days}\,\mathrm{decade}^{-1}$), but not in the UT ($-3.3 \pm 4.1\,\mathrm{days}\,\mathrm{decade}^{-1}$). The difference in the seasonal shift between the LT and the UT is also significant. Note that reducing the width of the time windows (to less than 9 years) does not give significantly different results.

At the three continental sites, Parrish et al. (2013) reported statistically significant rates of shift (at the 95 % confidence

Table 2. Characteristics of the O$_3$ seasonal cycle over the periods 1995–2003 and 2004–2012 in all tropospheric layers. Amplitude and phase are obtained by fitting a sine function to the daily mean O$_3$ mixing ratios (see text).

Layer	Amplitude			Phase		
	Amplitude 1995–2003 (ppb)	Amplitude 2004–2012 (ppb)	Amplitude trend (ppb decade^{-1})	Date of seasonal maximum 1995–2003	Date of seasonal maximum 2004–2012	Shift (day decade^{-1})
UT	18.0 ± 0.8	16.1 ± 0.7	-2.1 ± 1.2	23 June ± 2.6 days	20 June ± 2.6 days	-3.3 ± 4.1
MT	11.5 ± 0.5	10.5 ± 0.5	-1.1 ± 0.8	23 June ± 2.4 days	16 June ± 2.9 days	-7.8 ± 4.2
LT	9.9 ± 1.0	7.6 ± 1.1	-2.5 ± 1.7	18 June ± 5.8 days	2 June ± 8.6 days	-17.8 ± 11.5

level) ranging between -5 and -7 days decade^{-1} since the 1970s, while at the coastal site Mace Head, the rate was lower and insignificant (-3 ± 3.7 days decade^{-1}). In comparison, the seasonal shift we obtained in the LT is significantly higher, but discrepancies are likely due to the fact that the studied periods are different. As a faster change of phase is found between 2005 and 2008 (the last 3 years studied) (see Fig. 2 in Parrish et al., 2013), restricting their analysis to our shorter period would likely have led to a higher seasonal shift (i.e. closer to our values).

3.4.2 Discussion

The previous analysis confirms that the ozone seasonal pattern in central/western Europe has been changing, at least since the mid-1990s, moving toward a lower amplitude and an earlier O$_3$ maximum. It is worth noting that the MOZAIC–IAGOS observations above Frankfurt/Munich represent the densest data set of O$_3$ vertical profiles worldwide. The vertical profile observations provide unique data, allowing us to show that this seasonal change of the phase in the O$_3$ maximum to earlier days in the year extends above the surface at Frankfurt/Munich. The magnitude of this shift in maximum is statistically significant through the mid-troposphere. This may highlight that the O$_3$ seasonal pattern behaves differently over the Northern Hemispheric continents (Europe, North America, Asia). Indeed, the FLEXPART-derived PES clearly shows that the air masses sampled by MOZAIC–IAGOS aircraft in the different tropospheric layers originate from different regions (see Fig. 2). The LT is predominantly influenced by the European emissions, the MT by both the European and Northern American emissions, the UT by both the Northern American and Asian emissions.

Parrish et al. (2013) exhaustively discussed several reasons that may explain this changing phase at the surface in Europe, including changes in downward transport of stratospheric O$_3$, long-range transport, O$_3$ precursor's emissions and their spatial distribution, photochemical production and the potential influence of climate change. Our study does not provide an unambiguous explanation for either the seasonal trend discrepancies or the subsequent seasonal shifts (which would ideally require the use of global models able

to correctly reproduce both O$_3$ seasonal patterns and trends throughout the troposphere). In terms of stratospheric contributions, the STE is known to peak in spring (Auvray and Bey, 2005; James et al., 2003; Tang et al., 2011) due to both enhanced downward transport (Appenzeller et al., 1996) and maximum mixing ratios in the lowermost stratosphere (e.g. Thouret et al., 2006). If the seasonal shift was induced by higher STT fluxes, one would expect stronger positive trends in spring close to the tropopause compared to the LT and a larger (and more significant) seasonal shift in the UT, which contradicts our observations. Thus, the STE is not likely the main reason for the shift of the O$_3$ seasonal pattern. The trend analysis (Sect. 3.3) has not highlighted any significant O$_3$ trend either in spring or summer, the large uncertainties being at least partly due to the strong interannual variability of O$_3$ mixing ratios.

4 Summary and conclusions

Extensive databases of O$_3$ and CO vertical profiles above worldwide airports have been available from the MOZAIC–IAGOS programme since 1994 and 2002, respectively. In this study, we investigate the climatology, variations and trends of O$_3$ and CO mixing ratios above the German airports Frankfurt and Munich, which combined represent the densest and longest MOZAIC–IAGOS data set worldwide. We focus on the troposphere, with each vertical profile subdivided in three tropospheric layers: the lower, middle and upper troposphere (LT, MT and UT). The UT is defined relative to the dynamical tropopause, based on the potential vorticity extracted from ECMWF meteorological data. The main results are given below (all trends are given with uncertainties at a 95 % confidence level).

1. Climatological vertical profiles: the mean O$_3$ vertical profile is characterised by a strong increase with altitude in the first kilometre above the surface in any season and close to the tropopause in spring/summer, while the vertical gradient remains moderate (low) in the free troposphere in spring/summer (winter/autumn). These variations of the O$_3$ vertical gradient are likely due to the effect of deposition and titration by NO close to the surface and STE close to the tropopause. We also high-

lighted a minimum of daily O$_3$ variability at around 3–4 km. The mean CO vertical profile shows maximum mixing ratios at the surface, a strong decrease in the first kilometre (in particular in winter/autumn) and a moderate one in the rest of the troposphere. The day-to-day variability maximises at the surface, but remains constant (around 18 %) throughout the rest of the troposphere, regardless of the season.

2. Seasonal variations: the mean O$_3$ seasonal variations show a minimum in November–December in all tropospheric layers, a broad spring/summer maximum in the LT and MT and a sharper summer maximum in the UT. The O$_3$ 5th percentile is also minimum in November–December in the entire troposphere, but reaches its maximum in April–May in the LT and MT and April–August in the UT. The seasonal profile of the O$_3$ 95th percentile is less contrasted in the troposphere, with a maximum in April–August in the LT, July–August in the MT and May–July in the UT. The mean CO seasonal variations peak in March/April in the whole troposphere and reach a broad minimum in July–October in the LT, refined to September–October in the MT and UT. A similar pattern is observed for the CO 5th and 95th percentiles.

3. Annual and seasonal O$_3$ trends: over the period 1994–2012, most O$_3$ trends are insignificant. The few exceptions are the significant increases of the mean O$_3$ in winter and of the O$_3$ 5th percentile at the annual scale. No significant trends are found for the O$_3$ 95th percentile. Considering the uncertainties at a 95 % confidence level, the significant trend values range between 0.02 and 1.67 %O$_{3,2000}$ yr^{-1} (relative change with the year 2000 as a reference). Over the period 2002–2012, the mean CO mixing ratios decrease at the annual scale and at the seasonal scale in winter, spring and summer in all tropospheric layers (except in the LT in winter), with trends ranging between -2.31 [-3.61; -0.97] and -1.36 [-2.05; -0.74] %CO$_{2004}$ yr^{-1} (relative change with the year 2004 as a reference). A similar picture is observed for both the 5th and the 95th percentiles, except that most trends in spring and summer are insignificant for the 5th percentile. All trends remain insignificant in autumn.

This study also investigates the changes in the O$_3$ seasonal cycle (by fitting sinusoids over the 9-years periods 1995–2003 and 2004–2012) with a focus on the phase. Our results highlight a statistically significant change of the phase in the LT, with ozone maxima occurring earlier by -17.8 ± 11.5 days decade^{-1} on average (at a 95 % confidence level), in general agreement with previous results Parrish et al., 2013). A major contribution of this study is that it extends the analysis throughout the troposphere and shows that such shifts become smaller and less significant as one ap-

proaches the tropopause. In particular, the difference in seasonal shift between the LT and UT is statistically significant. The larger contribution from other regions (e.g. Asia) higher in altitude may explain the lower seasonal shift observed in the free troposphere and close to the tropopause, although further studies are required to quantitatively assess this issue.

5 Data availability

No new measurements were made for this review article. All ozone and carbon monoxide data sets mentioned in the text were obtained from the existing MOZAIC-IAGOS database, freely available on http://www.iagos.fr (IAGOS, 2016) or via the AERIS web site http://www.aeris-data.fr (AERIS, 2016).

The Supplement related to this article is available online at doi:10.5194/acp-16-15147-2016-supplement.

References

AERIS: Ozone and carbon monoxide datasets, available at: http://www.aeris-data.fr, last access: 17 November 2016.

Appenzeller, C., Holton, J. R., and Rosenlof, K. H.: Seasonal variation of mass transport across the tropopause, J. Geophys. Res.-Atmos., 101, 15071–15078, doi:10.1029/96JD00821, 1996.

Ashmore, M. R.: Assessing the future global impacts of ozone on vegetation, Plant Cell Environ., 28, 949–964, doi:10.1111/j.1365-3040.2005.01341.x, 2005.

Auvray, M. and Bey, I.: Long-range transport to Europe: Seasonal variations and implications for the European ozone budget, J. Geophys. Res., 110, D11303, doi:10.1029/2004JD005503, 2005.

Bethan, S., Vaughan, G., and Reid, S. J.: A comparison of ozone and thermal tropopause heights and the impact of tropopause definition on quantifying the ozone content of the troposphere, Q. J. Roy. Meteorol. Soc., 122, 929–944, doi:10.1002/qj.49712253207, 1996.

Carslaw, D. C. and Ropkins, K.: openair – An R package for air quality data analysis, Environ. Modell. Softw., 27–28, 52–61, doi:10.1016/j.envsoft.2011.09.008, 2012.

Cattiaux, J., Vautard, R., Cassou, C., Yiou, P., Masson-Delmotte, V., and Codron, F.: Winter 2010 in Europe: A cold extreme in a warming climate, Geophys. Res. Lett., 37, L20704, doi:10.1029/2010GL044613, 2010.

Chevalier, A., Gheusi, F., Delmas, R., Ordóñez, C., Sarrat, C., Zbinden, R., Thouret, V., Athier, G., and Cousin, J.-M.: Influence of altitude on ozone levels and variability in the lower troposphere: a ground-based study for western Europe over the period 2001–2004, Atmos. Chem. Phys., 7, 4311–4326, doi:10.5194/acp-7-4311-2007, 2007.

Cooper, O. R., Parrish, D. D., Ziemke, J., Balashov, N. V., Cupeiro, M., Galbally, I. E., Gilge, S., Horowitz, L., Jensen, N. R., Lamarque, J.-F., Naik, V., Oltmans, S. J., Schwab, J., Shindell, D. T., Thompson, A. M., Thouret, V., Wang, Y., and Zbinden, R. M.: Global distribution and trends of tropospheric ozone: An observation-based review, Elem. Sci. Anthr., 2, 000029, doi:10.12952/journal.elementa.000029, 2014.

Cui, J., Pandey Deolal, S., Sprenger, M., Henne, S., Staehelin, J., Steinbacher, M., and Nédélec, P.: Free tropospheric ozone changes over Europe as observed at Jungfraujoch (1990–2008): An analysis based on backward trajectories, J. Geophys. Res., 116, D10304, doi:10.1029/2010JD015154, 2011.

Derwent, R. G., Simmonds, P. G., Seuring, S., and Dimmer, C.: Observation and interpretation of the seasonal cycles in the surface concentrations of ozone and carbon monoxide at mace head, Ireland from 1990 to 1994, Atmos. Environ., 32, 145–157, doi:10.1016/S1352-2310(97)00338-5, 1998.

Derwent, R. G., Manning, A. J., Simmonds, P. G., Spain, T. G., and O'Doherty, S.: Analysis and interpretation of 25 years of ozone observations at the Mace Head Atmospheric Research Station on the Atlantic Ocean coast of Ireland from 1987 to 2012, Atmos. Environ., 80, 361–368, doi:10.1016/j.atmosenv.2013.08.003, 2013.

Dils, B., Cui, J., Henne, S., Mahieu, E., Steinbacher, M., and De Mazière, M.: 1997–2007 CO trend at the high Alpine site Jungfraujoch: a comparison between NDIR surface in situ and FTIR remote sensing observations, Atmos. Chem. Phys., 11, 6735–6748, doi:10.5194/acp-11-6735-2011, 2011.

Ding, A. J., Wang, T., Thouret, V., Cammas, J.-P., and Nédélec, P.: Tropospheric ozone climatology over Beijing: analysis of aircraft data from the MOZAIC program, Atmos. Chem. Phys., 8, 1–13, doi:10.5194/acp-8-1-2008, 2008.

Dueñas, C., Fernandez, M. C., Caete, S., Carretero, J., and Liger, É.: Assessment of ozone variations and meteorological effects in an urban area in the Mediterranean Coast, Sci. Total Environ., 299, 97–113, doi:10.1016/S0048-9697(02)00251-6, 2002.

Edwards, D. P., Emmons, L. K., Hauglustaine, D. A., Chu, D. A., Gille, J. C., Kaufman, Y. J., Pétron, G. P., Yurganov, L. N., Giglio, L., Deeter, M. N., Yudin, V., Ziskin, D. C., Warner, J., Lamarque, J.-F., Francis, G. L., Ho, S. P., Mao, D., Chen, J., Grechko, E. I., and Drummond, J. R.: Observations of carbon monoxide and aerosols from the Terra satellite: Northern Hemisphere variability, J. Geophys. Res., 109, D24202, doi:10.1029/2004JD004727, 2004.

Gaudel, A., Ancellet, G., and Godin-Beekmann, S.: Analysis of 20 years of tropospheric ozone vertical profiles by lidar and ECC

at Observatoire de Haute Provence (OHP) at 44° N, 6.7° E, Atmos. Environ., 113, 78–89, doi:10.1016/j.atmosenv.2015.04.028, 2015.

Gilge, S., Plass-Duelmer, C., Fricke, W., Kaiser, A., Ries, L., Buchmann, B., and Steinbacher, M.: Ozone, carbon monoxide and nitrogen oxides time series at four alpine GAW mountain stations in central Europe, Atmos. Chem. Phys., 10, 12295–12316, doi:10.5194/acp-10-12295-2010, 2010.

Hu, S., Fruin, S., Kozawa, K., Mara, S., Winer, A. M., and Paulson, S. E.: Aircraft Emission Impacts in a Neighborhood Adjacent to a General Aviation Airport in Southern California, Environ. Sci. Technol., 43, 8039–8045, doi:10.1021/es900975f, 2009.

IAGOS: Ozone and carbon monoxide datasets, available at: http://www.iagos.fr, last access: 17 November 2016.

IPCC: Climate Change 2007: The Physical Science Basis, Contribution of Working Group I to the Fourth Assessment Report of the Intergovernmental Panel on Climate Change; Intergovernmental Panel on Climate Change: Cambridge, UK and New York, NY, 2007, available at: http://www.ipcc.ch/publications_and_data/ar4/wg1/en/contents.html, 2013.

James, P., Stohl, A., Forster, C., Eckhardt, S., Seibert, P., and Frank, A.: A 15-year climatology of stratosphere-troposphere exchange with a Lagrangian particle dispersion model: 1. Methodology and validation, J. Geophys. Res., 108, 8519, doi:10.1029/2002JD002637, 2003.

Jerrett, M., Burnett, R. T., Pope, C. A., Ito, K., Thurston, G., Krewski, D., Shi, Y., Calle, E., and Thun, M.: Long-term ozone exposure and mortality, New Engl. J. Med., 360, 1085–95, doi:10.1056/NEJMoa0803894, 2009.

Junge, C. E.: Residence time and variability of tropospheric trace gases, Tellus, 26, 477–488, doi:10.1111/j.2153-3490.1974.tb01625.x, 1974.

Karlsdóttir, S., Isaksen, I. S. A., Myhre, G., and Berntsen, T. K.: Trend analysis of O$_3$ and CO in the period 1980–1996: A three-dimensional model study, J. Geophys. Res., 105, 28907, doi:10.1029/2000JD900374, 2000.

Kesgin, U.: Aircraft emissions at Turkish airports, Energy, 31, 372–384, doi:10.1016/j.energy.2005.01.012, 2006.

Koumoutsaris, S., Bey, I., Generoso, S., and Thouret, V.: Influence of El Niño–Southern Oscillation on the interannual variability of tropospheric ozone in the northern midlatitudes, J. Geophys. Res., 113, D19301, doi:10.1029/2007JD009753, 2008.

Kunz, A., Konopka, P., Müller, R., and Pan, L. L.: Dynamical tropopause based on isentropic potential vorticity gradients, J. Geophys. Res., 116, D01110, doi:10.1029/2010JD014343, 2011.

Kurniawan, J. S. and Khardi, S.: Comparison of methodologies estimating emissions of aircraft pollutants, environmental impact assessment around airports, Environ. Impact Asses., 31, 240–252, doi:10.1016/j.eiar.2010.09.001, 2011.

Logan, J. A., Megretskaia, I. A., Miller, A. J., Tiao, G. C., Choi, D., Zhang, L., Stolarski, R. S., Labow, G. J., Hollandsworth, S. M., Bodeker, G. E., Claude, H., De Muer, D., Kerr, J. B., Tarasick, D. W., Oltmans, S. J., Johnson, B., Schmidlin, F., Staehelin, J., Viatte, P., and Uchino, O.: Trends in the vertical distribution of ozone: A comparison of two analyses of ozonesonde data, J. Geophys. Res., 104, 26373, doi:10.1029/1999JD900300, 1999.

Logan, J. A., Staehelin, J., Megretskaia, I. A., Cammas, J.-P., Thouret, V., Claude, H., De Backer, H., Steinbacher, M., Scheel, H.-E., Stübi, R., Fröhlich, M., and Derwent, R.: Changes in

ozone over Europe: Analysis of ozone measurements from sondes, regular aircraft (MOZAIC) and alpine surface sites, J. Geophys. Res., 117, D09301, doi:10.1029/2011JD016952, 2012.

Marenco, A., Thouret, V., Nédélec, P., Smit, H., Helten, M., Kley, D., Karcher, F., Simon, P., Law, K., Pyle, J., Poschmann, G., Von Wrede, R., Hume, C., and Cook, T.: Measurement of ozone and water vapor by Airbus in-service aircraft: The MOZAIC airborne program, an overview, J. Geophys. Res.-Atmos., 103, 25631–25642, doi:10.1029/98JD00977, 1998.

Meleux, F., Solmon, F., and Giorgi, F.: Increase in summer European ozone amounts due to climate change, Atmos. Environ., 41, 7577–7587, doi:10.1016/j.atmosenv.2007.05.048, 2007.

Moise, T. and Rudich, Y.: Reactive uptake of ozone by proxies for organic aerosols: Surface versus bulk processes, J. Geophys. Res., 105, 14667, doi:10.1029/2000JD900071, 2000.

Moise, T. and Rudich, Y.: Reactive Uptake of Ozone by Aerosol-Associated Unsaturated Fatty Acids: Kinetics, Mechanism, and Products, J. Phys. Chem. A, 106, 6469–6476, doi:10.1021/jp025597e, 2002.

Nedelec, P., Cammas, J.-P., Thouret, V., Athier, G., Cousin, J.-M., Legrand, C., Abonnel, C., Lecoeur, F., Cayez, G., and Marizy, C.: An improved infrared carbon monoxide analyser for routine measurements aboard commercial Airbus aircraft: technical validation and first scientific results of the MOZAIC III programme, Atmos. Chem. Phys., 3, 1551–1564, doi:10.5194/acp-3-1551-2003, 2003.

Nédélec, P., Blot, R., Boulanger, D., Athier, G., Cousin, J.-M., Gautron, B., Petzold, A., Volz-Thomas, A., and Thouret, V.: Instrumentation on commercial aircraft for monitoring the atmospheric composition on a global scale: the IAGOS system, technical overview of ozone and carbon monoxide measurements, Tellus B, 67, 1–16, doi:10.3402/tellusb.v67.27791, 2015.

Novelli, P. C., Masarie, K. A., Lang, P. M., Hall, B. D., Myers, R. C., and Elkins, J. W.: Reanalysis of tropospheric CO trends: Effects of the 1997–1998 wildfires, J. Geophys. Res., 108, 4464, doi:10.1029/2002JD003031, 2003.

Oltmans, S. J., Lefohn, A. S., Scheel, H. E., Harris, J. M., Levy, H., Galbally, I. E., Brunke, E.-G., Meyer, C. P., Lathrop, J. A., Johnson, B. J., Shadwick, D. S., Cuevas, E., Schmidlin, F. J., Tarasick, D. W., Claude, H., Kerr, J. B., Uchino, O., and Mohnen, V.: Trends of ozone in the troposphere, Geophys. Res. Lett., 25, 139–142, doi:10.1029/97GL03505, 1998.

Oltmans, S. J., Lefohn, A. S., Harris, J. M., Galbally, I., Scheel, H. E., Bodeker, G., Brunke, E., Claude, H., Tarasick, D., Johnson, B. J., Simmonds, P., Shadwick, D., Anlauf, K., Hayden, K., Schmidlin, F., Fujimoto, T., Akagi, K., Meyer, C., Nichol, S., Davies, J., Redondas, A., and Cuevas, E.: Long-term changes in tropospheric ozone, Atmos. Environ., 40, 3156–3173, doi:10.1016/j.atmosenv.2006.01.029, 2006.

Oltmans, S. J., Lefohn, A. S., Shadwick, D., Harris, J. M., Scheel, H. E., Galbally, I., Tarasick, D. W., Johnson, B. J., Brunke, E.-G., Claude, H., Zeng, G., Nichol, S., Schmidlin, F., Davies, J., Cuevas, E., Redondas, A., Naoe, H., Nakano, T., and Kawasato, T.: Recent tropospheric ozone changes – A pattern dominated by slow or no growth, Atmos. Environ., 67, 331–351, doi:10.1016/j.atmosenv.2012.10.057, 2013.

Ordóñez, C., Mathis, H., Furger, M., Henne, S., Hüglin, C., Staehelin, J., and Prévôt, A. S. H.: Changes of daily surface ozone maxima in Switzerland in all seasons from 1992 to 2002 and discussion of summer 2003, Atmos. Chem. Phys., 5, 1187–1203, doi:10.5194/acp-5-1187-2005, 2005.

Paoletti, E.: Impact of ozone on Mediterranean forests: a review, Environ. Pollut., 144, 463–74, doi:10.1016/j.envpol.2005.12.051, 2006.

Parrish, D. D., Law, K. S., Staehelin, J., Derwent, R., Cooper, O. R., Tanimoto, H., Volz-Thomas, A., Gilge, S., Scheel, H.-E., Steinbacher, M., and Chan, E.: Long-term changes in lower tropospheric baseline ozone concentrations at northern mid-latitudes, Atmos. Chem. Phys., 12, 11485–11504, doi:10.5194/acp-12-11485-2012, 2012.

Parrish, D. D., Law, K. S., Staehelin, J., Derwent, R., Cooper, O. R., Tanimoto, H., Volz-Thomas, A., Gilge, S., Scheel, H.-E., Steinbacher, M., and Chan, E.: Lower tropospheric ozone at northern midlatitudes: Changing seasonal cycle, Geophys. Res. Lett., 40, 1631–1636, doi:10.1002/grl.50303, 2013.

Parrish, D. D., Lamarque, J.-F., Naik, V., Horowitz, L., Shindell, D. T., Staehelin, J., Derwent, R., Cooper, O. R., Tanimoto, H., Volz-Thomas, A., Gilge, S., Scheel, H.-E., Steinbacher, M., and Fröhlich, M.: Long-term changes in lower tropospheric baseline ozone concentrations: Comparing chemistry-climate models and observations at northern midlatitudes, J. Geophys. Res.-Atmos., 119, 5719–5736, doi:10.1002/2013JD021435, 2014.

Petetin, H., Thouret, V., Athier, G., Blot, R., Boulanger, D., Cousin, J.-M., Gaudel, A., Nédélec, P., and Cooper, O.: Diurnal cycle of ozone throughout the troposphere over Frankfurt as measured by MOZAIC-IAGOS commercial aircraft, Elem. Sci. Anthr., 4, 1–11, doi:10.12952/journal.elementa.000129, 2016.

Petzold, A., Thouret, V., Gerbig, C., Zahn, A., Brenninkmeijer, C. A. M., Gallagher, M., Hermann, M., Pontaud, M., Ziereis, H., Boulanger, D., Marshall, J., Nédélec, P., Smit, H. G. J., Friess, U., Flaud, J.-M., Wahner, A., Cammas, J.-P., and Volz-Thomas, A.: Global-scale atmosphere monitoring by in-service aircraft – current achievements and future prospects of the European Research Infrastructure IAGOS, Tellus B, 67, 1–24, doi:10.3402/tellusb.v67.28452, 2015.

Pison, I. and Menut, L.: Quantification of the impact of aircraft traffic emissions on tropospheric ozone over Paris area, Atmos. Environ., 38, 971–983, doi:10.1016/j.atmosenv.2003.10.056, 2004.

Sen, P. K.: Estimates of the Regression Coefficient Based on Kendall's Tau, J. Am. Stat. Assoc., 63, 1379–1389, doi:10.1080/01621459.1968.10480934, 1968.

Simmonds, P. G., Derwent, R. G., Manning, A. L., and Spain, G.: Significant growth in surface ozone at Mace Head, Ireland, 1987–2003, Atmos. Environ., 38, 4769–4778, doi:10.1016/j.atmosenv.2004.04.036, 2004.

Solberg, S., Hov, Ø., Søvde, A., Isaksen, I. S. A., Coddeville, P., De Backer, H., Forster, C., Orsolini, Y., and Uhse, K.: European surface ozone in the extreme summer 2003, J. Geophys. Res., 113, D07307, doi:10.1029/2007JD009098, 2008.

Staufer, J., Staehelin, J., Stübi, R., Peter, T., Tummon, F., and Thouret, V.: Trajectory matching of ozonesondes and MOZAIC measurements in the UTLS – Part 1: Method description and application at Payerne, Switzerland, Atmos. Meas. Tech., 6, 3393–3406, doi:10.5194/amt-6-3393-2013, 2013.

Staufer, J., Staehelin, J., Stübi, R., Peter, T., Tummon, F., and Thouret, V.: Trajectory matching of ozonesondes and MOZAIC measurements in the UTLS – Part 2: Application to the

global ozonesonde network, Atmos. Meas. Tech., 7, 241–266, doi:10.5194/amt-7-241-2014, 2014.

Stevenson, D. S., Dentener, F. J., Schultz, M. G., Ellingsen, K., van Noije, T. P. C., Wild, O., Zeng, G., Amann, M., Atherton, C. S., Bell, N., Bergmann, D. J., Bey, I., Butler, T., Cofala, J., Collins, W. J., Derwent, R. G., Doherty, R. M., Drevet, J., Eskes, H. J., Fiore, A. M., Gauss, M., Hauglustaine, D. A., Horowitz, L. W., Isaksen, I. S. A., Krol, M. C., Lamarque, J.-F., Lawrence, M. G., Montanaro, V., Müller, J.-F., Pitari, G., Prather, M. J., Pyle, J. A., Rast, S., Rodriguez, J. M., Sanderson, M. G., Savage, N. H., Shindell, D. T., Strahan, S. E., Sudo, K., and Szopa, S.: Multimodel ensemble simulations of present-day and near-future tropospheric ozone, J. Geophys. Res., 111, D08301, doi:10.1029/2005JD006338, 2006.

Stohl, A., Forster, C., Eckhardt, S., Spichtinger, N., Huntrieser, H., Heland, J., Schlager, H., Wilhelm, S., Arnold, F., and Cooper, O.: A backward modeling study of intercontinental pollution transport using aircraft measurements, J. Geophys. Res., 108, 4370, doi:10.1029/2002JD002862, 2003a.

Stohl, A., Wernli, H., James, P., Bourqui, M., Forster, C., Liniger, M. A., Seibert, P., and Sprenger, M.: A New Perspective of Stratosphere–Troposphere Exchange, B. Am. Meteorol. Soc., 84, 1565–1573, doi:10.1175/BAMS-84-11-1565, 2003b.

Stohl, A., Forster, C., Frank, A., Seibert, P., and Wotawa, G.: Technical note: The Lagrangian particle dispersion model FLEXPART version 6.2, Atmos. Chem. Phys., 5, 2461–2474, doi:10.5194/acp-5-2461-2005, 2005.

Struzewska, J. and Kaminski, J. W.: Formation and transport of photooxidants over Europe during the July 2006 heat wave – observations and GEM-AQ model simulations, Atmos. Chem. Phys., 8, 721–736, doi:10.5194/acp-8-721-2008, 2008.

Tang, Q., Prather, M. J., and Hsu, J.: Stratosphere-troposphere exchange ozone flux related to deep convection, Geophys. Res. Lett., 38, L03806, doi:10.1029/2010GL046039, 2011.

Tanimoto, H., Zbinden, R. M., Thouret, V., and Nédélec, P.: Consistency of tropospheric ozone observations made by different platforms and techniques in the global databases, Tellus B, 67, 27073, doi:10.3402/tellusb.v67.27073, 2015.

Thouret, V., Marenco, A., Logan, J. A., Nédélec, P., and Grouhel, C.: Comparisons of ozone measurements from the MOZAIC airborne program and the ozone sounding network at eight locations, J. Geophys. Res., 103, 25695–25720, doi:10.1029/98JD02243, 1998.

Thouret, V., Cammas, J.-P., Sauvage, B., Athier, G., Zbinden, R., Nédélec, P., Simon, P., and Karcher, F.: Tropopause referenced ozone climatology and inter-annual variability (1994–2003) from the MOZAIC programme, Atmos. Chem. Phys., 6, 1033–1051, doi:10.5194/acp-6-1033-2006, 2006.

Tiao, G. C., Reinsel, G. C., Pedrick, J. H., Allenby, G. M., Mateer, C. L., Miller, A. J., and DeLuisi, J. J.: A statistical trend analysis of ozonesonde data, J. Geophys. Res., 91, 13121, doi:10.1029/JD091iD12p13121, 1986.

Tressol, M., Ordonez, C., Zbinden, R., Brioude, J., Thouret, V., Mari, C., Nedelec, P., Cammas, J.-P., Smit, H., Patz, H.-W., and Volz-Thomas, A.: Air pollution during the 2003 European heat wave as seen by MOZAIC airliners, Atmos. Chem. Phys., 8, 2133–2150, doi:10.5194/acp-8-2133-2008, 2008.

Vautard, R., Beekmann, M., Roux, J., and Gombert, D.: Validation of a hybrid forecasting system for the ozone concen-

trations over the Paris area, Atmos. Environ., 35, 2449–2461, doi:10.1016/S1352-2310(00)00466-0, 2001.

Van Dingenen, R., Dentener, F. J., Raes, F., Krol, M. C., Emberson, L., and Cofala, J.: The global impact of ozone on agricultural crop yields under current and future air quality legislation, Atmos. Environ., 43, 604–618, doi:10.1016/j.atmosenv.2008.10.033, 2009.

van Loon, M., Vautard, R., Schaap, M., Bergström, R., Bessagnet, B., Brandt, J., Builtjes, P. J. H., Christensen, J. H., Cuvelier, C., Graff, A., Jonson, J. E., Krol, M., Langner, J., Roberts, P., Rouil, L., Stern, R., Tarrasón, L., Thunis, P., Vignati, E., White, L., and Wind, P.: Evaluation of long-term ozone simulations from seven regional air quality models and their ensemble, Atmos. Environ., 41, 2083–2097, doi:10.1016/j.atmosenv.2006.10.073, 2007.

Weatherhead, E. C., Stevermer, A. J., and Schwartz, B. E.: Detecting environmental changes and trends, Phys. Chem. Earth, 27, 399–403, doi:10.1016/S1474-7065(02)00019-0, 2002.

Wilks, D. S.: Statistical Methods in the Atmospheric Sciences, 2nd edition, Academic P., San Diego, USA, 2006.

Wilson, R. C., Fleming, Z. L., Monks, P. S., Clain, G., Henne, S., Konovalov, I. B., Szopa, S., and Menut, L.: Have primary emission reduction measures reduced ozone across Europe? An analysis of European rural background ozone trends 1996–2005, Atmos. Chem. Phys., 12, 437–454, doi:10.5194/acp-12-437-2012, 2012.

Worden, H. M., Deeter, M. N., Frankenberg, C., George, M., Nichitiu, F., Worden, J., Aben, I., Bowman, K. W., Clerbaux, C., Coheur, P. F., de Laat, A. T. J., Detweiler, R., Drummond, J. R., Edwards, D. P., Gille, J. C., Hurtmans, D., Luo, M., Martínez-Alonso, S., Massie, S., Pfister, G., and Warner, J. X.: Decadal record of satellite carbon monoxide observations, Atmos. Chem. Phys., 13, 837–850, doi:10.5194/acp-13-837-2013, 2013.

Wu, S., Mickley, L. J., Jacob, D. J., Logan, J. A., Yantosca, R. M., and Rind, D.: Why are there large differences between models in global budgets of tropospheric ozone?, J. Geophys. Res., 112, D05302, doi:10.1029/2006JD007801, 2007.

Yu, K. N., Cheung, Y. P., Cheung, T., and Henry, R. C.: Identifying the impact of large urban airports on local air quality by nonparametric regression, Atmos. Environ., 38, 4501–4507, doi:10.1016/j.atmosenv.2004.05.034, 2004.

Zahn, A., Brenninkmeijer, C. A. M., Asman, W. A. H., Crutzen, P. J., Heinrich, G., Fischer, H., Cuijpers, J. W. M., and van Velthoven, P. F. J.: The budgets of O$_3$ and CO in the upper troposphere: CARIBIC passenger aircraft results 1997–2001, J. Geophys. Res., 107, 4337, doi:10.1029/2001JD001529, 2002.

Zbinden, R. M., Cammas, J.-P., Thouret, V., Nédélec, P., Karcher, F., and Simon, P.: Mid-latitude tropospheric ozone columns from the MOZAIC program: climatology and interannual variability, Atmos. Chem. Phys., 6, 1053–1073, doi:10.5194/acp-6-1053-2006, 2006.

Zbinden, R. M., Thouret, V., Ricaud, P., Carminati, F., Cammas, J.-P., and Nédélec, P.: Climatology of pure tropospheric profiles and column contents of ozone and carbon monoxide using MOZAIC in the mid-northern latitudes (24° N to 50° N) from 1994 to 2009, Atmos. Chem. Phys., 13, 12363–12388, doi:10.5194/acp-13-12363-2013, 2013.

Zellweger, C., Hüglin, C., Klausen, J., Steinbacher, M., Vollmer, M., and Buchmann, B.: Inter-comparison of four different carbon monoxide measurement techniques and evaluation of the

long-term carbon monoxide time series of Jungfraujoch, At-
mos. Chem. Phys., 9, 3491–3503, doi:10.5194/acp-9-3491-2009,
2009.

Zeng, G. and Pyle, J. A.: Influence of El Niño Southern Os-
cillation on stratosphere/troposphere exchange and the global
tropospheric ozone budget, Geophys. Res. Lett., 32, L01814,
doi:10.1029/2004GL021353, 2005.